Available online at www.sciencedirect.com
ScienceDirect
Advances in Space Research 46 (2010) 1218–1224
ADVANCES IN SPACE RESEARCH (a COSPAR publication)
www.elsevier.com/locate/asr

Network based real-time precise point positioning

Haojun Li [a], Junping Chen [b,*], Jiexian Wang [a,c], Congwei Hu [a,c], Zhiqiang Liu [a,d]

[a] Department of Surveying and Geo-Informatics Engineering, Tongji University, Shanghai 200092, PR China
[b] Deutsches GeoForschungsZentrum-GFZ, 14473 Potsdam, Germany
[c] Key Laboratory of Modern Engineering Surveying, State Bureau of Surveying and Mapping, Shanghai 200092, PR China
[d] College of Earth Science and Engineering, Hohai University, Nanjing 210098, PR China

Received 26 January 2010; received in revised form 3 June 2010; accepted 6 June 2010

Abstract

Network based real-time precise point positioning system includes two stages, i.e. real-time estimation of satellite clocks based on a reference network and real-time precise point positioning thereafter. In this paper, a satellite- and epoch-differenced approach, adopted from what is introduced by Han et al. (2001), is presented for the determination of satellite clocks and for the precise point positioning. One important refinement of our approach is the implementation of the robust clock estimation. A prototype software system is developed, and data from the European Reference Frame Permanent Network on September 19, 2009 is used to evaluate the approach. Results show that our approach is 3 times and 90 times faster than the epoch-difference approach and the zero-difference approach, respectively, which demonstrates a significant improvement in the computation efficiency. The RMS of the estimated clocks is at the level of 0.1 ns (3 cm) compared to the IGS final clocks. The clocks estimates are then applied to the precise point positioning in both kinematic and static mode. In static mode, the 2-h estimated coordinates have a mean accuracy of 3.08, 5.79, 6.32 cm in the North, East and Up directions. In kinematic mode, the mean kinematic coordinates accuracy is of 4.63, 5.82, 9.20 cm.

Keywords: Real-time precise point positioning; GNSS; Network-based positioning; Clock estimation

1. Introduction

Real-time kinematic (known as RTK) positioning is widely used in regional scale (e.g. Bock et al., 2000; Rizos, 2003; Rocken et al., 2004). The major restriction of the state-of-art network RTK systems is its rather short reference station spacing, usually in the range of 100 km or less. With future generation Global Navigation Satellite System (GNSS) signals and accurate ionospheric corrections, the distance may be extended (e.g. Hernandez-Pajares et al., 2004; Feng and Li, 2008).

On the other hand, Precise Point Positioning (PPP, Zumberge et al., 1997) has been demonstrated being a valuable technique for single stations positioning over continental even global scale (Kouba, 2005; Geng et al., 2009). Accuracy of satellite clocks and orbits are essential in the PPP based data analysis as they are fixed as known. In real-time positioning, while orbits are normally obtained from broadcast ephemeris in RTK, more accurate orbits need to be applied in real-time PPP. Currently, the International GNSS Service (IGS, Dow et al., 2005) provides Ultra-Rapid (IGU) orbits, which contain orbits of 48 h, where the first 24-h part is estimated and the later 24 h is predicted. The precision of the predicted orbits is around a few centimeters for the first 6 h (Hauschild et al., 2009; Dousa, 2009). However, current precision of the broadcast GPS clocks is roughly 5 ns (1.5 m) or 2 ns (0.6 m) of IGU clocks as monitored by the IGS (Senior et al., 2008).

* Corresponding author. Tel.: +49 (0)331 288 1199; fax: +49 (0)331 288 1759.
E-mail addresses: yanlhjch@126.com (H. Li), junping.chen@gfz-potsdam.de (J. Chen), wangjiexian@tongji.edu.cn (J. Wang), cwhu@tongji.edu.cn (C. Hu), zqliuer@hotmail.com (Z. Liu).

0273-1177/$36.00 © 2010 COSPAR. Published by Elsevier Ltd. All rights reserved.
doi:10.1016/j.asr.2010.06.015

Therefore the key problem for real-time PPP is the estimation of precise satellite clock corrections.

Satellite clock corrections are normally estimated from a reference network by batch processing in an iterative way. This procedure works in post-processing, however it is time consuming and difficult to meet the real-time requirements. The current real-time satellite clocks from different analysis centers of the IGS Real-time Pilot Project (IGS-RTPP, Caissy, 2006) are at the sampling of 5–30 s. For fast satellite clocks estimation, Han et al. (2001) present a time- and satellite-differenced method, which eliminates the ambiguities and receiver clock parameters. However, in their approach they apply equal weights in the estimation of satellite clocks, which means a problem from even one station in the reference network will ruin the results. To improve the reliability of the clock estimates, the robust estimation (Yang, 1999) is implemented in our approach. Another refinement to their approach is that tropospheric delays are being parameterized in the site positioning. The outline of this paper is as follows. In Section 2 the algorithm for the determination of real-time satellite- and epoch-differenced (SDED) satellite clocks is introduced. Section 3 concentrates on algorithm of the application of SDED clocks in PPP positioning. Then in Section 4, the prototype processing system is introduced. In Section 5 clock and PPP results are presented and discussed.

2. SDED satellite clocks estimation

Generally, the dual-frequency GNSS observables are used to eliminate the first-order ionospheric effects by the forming the ionosphere-free (L3) combinations. The L3 phase observation at station m follows (e.g. Xu, 2007):

$$L_m^j = \rho_m^j + c\cdot\delta_m - c\cdot\delta^j + b_m^j + T_m^j + \varepsilon(\Phi_{\mathrm{IF}})_m^j \tag{1}$$

The superscript j indicates tracked satellite; L_m^j is the ionosphere-free phase observation; ρ_m^j is the geometric range between receiver m and satellite j; δ_m is the receiver clock; δ^j is the satellite clock; c denotes the speed of light; b_m^j is the non-integer ambiguity of the ionosphere-free phase combination; T_m^j is the tropospheric delay; $\varepsilon(\Phi_{\mathrm{IF}})_m^j$ is the phase noise of combined observations.

For one receiver tracking two satellites (i, j) simultaneously, the single-differenced measurements between satellite can be used to eliminate the receiver clocks. By taking differences of L3 combinations of satellite i and j, we obtain

$$L_m^{j,i} = L_m^j - L_m^i = \rho_m^{j,i} - c\cdot\delta^{j,i} + b_m^{j,i} + T_m^{j,i} + \varepsilon(\Phi_{\mathrm{IF}})_m^{j,i} \tag{2}$$

Eq. (2) is the defined as the satellite-differenced (SD) equation and can be re-written as:

$$\delta^{j,i} = \frac{1}{c}\cdot\left(\rho_m^{j,i} + b_m^{j,i} + T_m^{j,i} - L_m^{j,i}\right) + \varepsilon(\Phi_{\mathrm{IF}})_m^{j,i} \tag{3}$$

where $\delta^{j,i}$ is called the SD clock. The superscript "j,i" indicates the differencing between satellite i and j, e.g. $L_m^{j,i} = L_m^j - L_m^i$.

Assuming there are no cycle slips between two adjacent epochs, the ambiguity term $b_m^{j,i}$ in Eq. (3) can be further eliminated by differencing the SD observations at the adjacent epoch n and $n-1$:

$$\begin{aligned}\Delta L_m^{j,i}(n) &= L_m^{j,i}(n) - L_m^{j,i}(n-1)\\ &= \Delta\rho_m^{j,i}(n) - c\cdot\Delta\delta_m^{j,i}(n) + \Delta T_m^{j,i}(n) + \Delta\varepsilon(\Phi_{\mathrm{IF}})_m^{j,i}\end{aligned} \tag{4}$$

Eq. (4) can be re-written as:

$$\Delta\delta_m^{j,i}(n) = \frac{1}{c}\cdot\left(\Delta\rho_m^{j,i}(n) + \Delta T_m^{j,i}(n) - \Delta L_m^{j,i}(n)\right) + \Delta\varepsilon(\Phi_{\mathrm{IF}})_m^{j,i} \tag{5}$$

where "Δ" indicates the epoch-difference (ED) operator and $\Delta\delta_m^{j,i}$ is defined as the SDED clock at station m.

For stations in a reference network, coordinates are precisely known and the geometric term in Eq. (5) can be precisely obtained. Tropospheric delay can be modeled using the Saastamoinen model, by which the most of the tropospheric delay is corrected. Janes et al. (1991) compare the tropospheric delay from Saastamoinen model and ray-tracing results at different locations and different seasons. They state the maximum difference is 48 mm at elevation of 10° and becomes smaller with the elevation increasing. By forming difference between adjacent epochs, which samples at 30 s or less, the difference will be then less than 1 mm. Therefore, tropospheric delay can be sufficiently corrected using the Saastamoinen model in our SDED approach. With coordinates fixed and tropospheric delay modeled, epoch-wise satellite clock can be estimated at each reference station based on Eq. (5). Assuming there are k reference stations in the network, which improves the redundancy of the solution, the final SDED satellite clock $\Delta\delta^{j,i}$ can be calculated by averaging $\Delta\delta_m^{j,i}$ over the network:

$$\Delta\delta^{j,i}(n) = \frac{1}{k}\cdot\sum_{m=1}^{k}\Delta\delta_m^{j,i} \tag{6}$$

To detect and remove the potential biases and outliers from some reference stations, the robust estimation (Yang, 1999) is used, where for each station m the weight function is as follows:

$$\bar{p}_m = \begin{cases} 1 & |V_m| \leqslant k_0 \\ \frac{k_0}{|V_m|}\left(\frac{k_1-|V_m|}{k_1-k_0}\right)^2 & k_0 < |V_m| \leqslant k_1 \\ 0 & |V_m| > k_1 \end{cases} \tag{7}$$

where $\bar{p}_m$ is the weight; $V_m = \frac{v_m}{\sigma_0}$ is a factor showing quantity of each residual v_m and σ_0 is the calculated variance factor; k_0 and k_1 are suitable constants which can be chosen by experiment or by the actual observation distribution. Following Yang (1999), we chose k_0 as 1.5 and k_1 as 3.0. And SDED clock can be computed by the following function:

$$\Delta\delta^{j,i}(n) = \sum_{m=1}^{k}\left(\Delta\delta_m^{j,i}(n)\cdot\bar{p}_m\right)\Big/\left(\sum_{m=1}^{k}\bar{p}_m\right) \tag{8}$$

Using SDED clock from our algorithm, the SD clock at epoch n can be expressed as:

$$\delta^{j,i}(n) = \delta^{j,i}(n_0) + \sum_{n_1=1}^{np} \Delta\delta^{j,i}(n_1) \tag{9}$$

where $\delta^{j,i}(n_0)$ is the SD clock at the reference epoch n_0, $\Delta\delta^{j,i}(n_1)$ is the SDED clock at epoch n_1 and np is the number of epochs between the reference epoch and epoch n. If the SD clock at the reference epoch is known, the SD clocks at all epochs can be computed by Eq. (9).

In the SDED approach, data analysis is performed station by station and only simple mathematic calculation is needed, which avoids the huge computation loads in the traditional approach. There is only one assumption that tropospheric delay can be calculated with conventional model and thus its temporal changes in a short interval can be ignored. The data preprocessing and outlier detection with the robust estimation technique is the key step to ensure the quality of the estimated clocks. The estimated clocks are relative clocks, whose absolute clocks depend on the SD clock at reference epoch. As a matter of fact, absolute clocks at all the other epochs will have the same bias. In the next section, we will show that this bias can be absorbed by ambiguities in PPP positioning.

3. PPP based real-time positioning

SDED clocks are relative clocks and therefore cannot be directly implement in traditional PPP algorithm. Substituting Eq. (9) into the SD equation (2), we get:

$$\rho_m^{j,i} - c \cdot \left(\delta^{j,i}(n_0) + \sum_{n_1=1}^{np} \Delta\delta^{j,i}(n_1) \right) + b_m^{j,i} + T_m^{j,i} = L_m^{j,i} - \varepsilon(\Phi_{\mathrm{IF}})_m^{j,i} \tag{10}$$

Considering SD clock $\delta^{j,i}(n_0)$ is a constant over time, we can define $N_m^{j,i} = b_m^{j,i} - c \cdot \delta^{j,i}(n_0)$ in Eq. (10), which is the new ambiguity namely pseudo-ambiguity. By further defining $L = L_m^{j,i} + c \cdot \sum_{n_1=1}^{np} \Delta\delta^{j,i}(n_1)$, Eq. (10) can be simplified as:

$$\rho_m^{j,i} + N_m^{j,i} + T_m^{j,i} = L - \varepsilon(\Phi_{\mathrm{IF}})_m^{j,i} \tag{11}$$

Eq. (11) is the modified PPP algorithm based on SD equation, the unknowns are station coordinates, pseudo-ambiguities, and zenith tropospheric delay (ZTD). The estimator of least-square adjustment or Kalman filter can be implemented to process the data.

4. The realization of network based real-time PPP service

Based on the SDED algorithm, prototype analysis system (NET–PPP) was developed. The structure of the system can be sketched as in Fig. 1.

The first step of the system, block "NET" in Fig. 1, is the estimation of SDED satellite clocks, where observations of reference stations are collected and used. The receiver related errors (e.g. receiver clocks, hardware delay, etc.) and ambiguities are eliminated by forming satellite- and epoch-difference. Redundant estimates of SDED satellite clocks can be obtained by implementing the robust estimation strategy. Due to the reduced number of parameters, the clock estimation can be done on epoch level and is capable for real-time application even for a huge network. In the second step, block "PPP" in Fig. 1, the SDED satellite clocks are then used at user stations for PPP based static or kinematic positioning using the modified PPP algorithm in Section 3. A Kalman filter is implemented in this step.

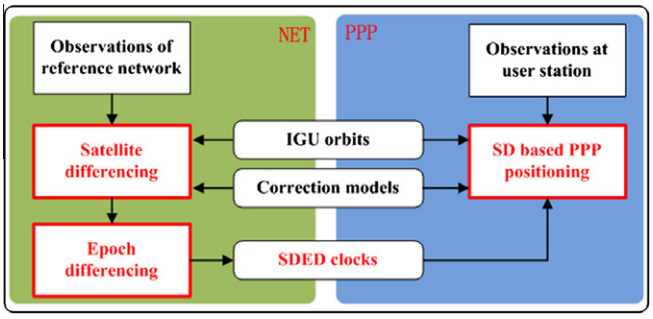

Fig. 1. Structure of the system NET–PPP.

In the estimation of SDED clocks, preprocessing of phase data is based on the Melbourne–Wuebbena combination. When cycle slips are detected, observations of corresponding satellite are then deleted. In both steps, IGU orbits are used and kept fixed. The same correction models including the phase wind-up, earth tides, relativistic effects, antenna phase center offset, variation, etc. are implemented according to IERS convention or IGS recommendation. Tropospheric delay is treated differently in the above two steps. It is corrected using the Saastamoinen model in SDED clock estimation. In PPP positioning, Saastamoinen model is used to get the a priori correction and the rest wet part is estimated by setting up a Piece Wise Constant (PWC) at an interval of 1 h.

5. Data processing

In the NET–PPP system, real-time data streaming part is still under development. To test the performance of our algorithm, we simulate a real-time experiment, where data is streamed based on daily files and analyzed in real-time-like epoch-wise mode. Fig. 2 shows a network of 52 stations from European Reference Frame (EUREF) Permanent Network (EPN) of which daily observations on September 19, 2009 are used for the determination of the SDED satellite clocks. The coordinates of the reference stations are fixed, and the IGU orbits and ERPs are fixed as well. To assess the precision of SDED clocks, we select nine test EPN stations, which are not used for the SDED clock determination, to conduct PPP positioning. PPP is performed in static and kinematic mode. In static mode, each daily file is split into 12 2-h sessions, which results in 12

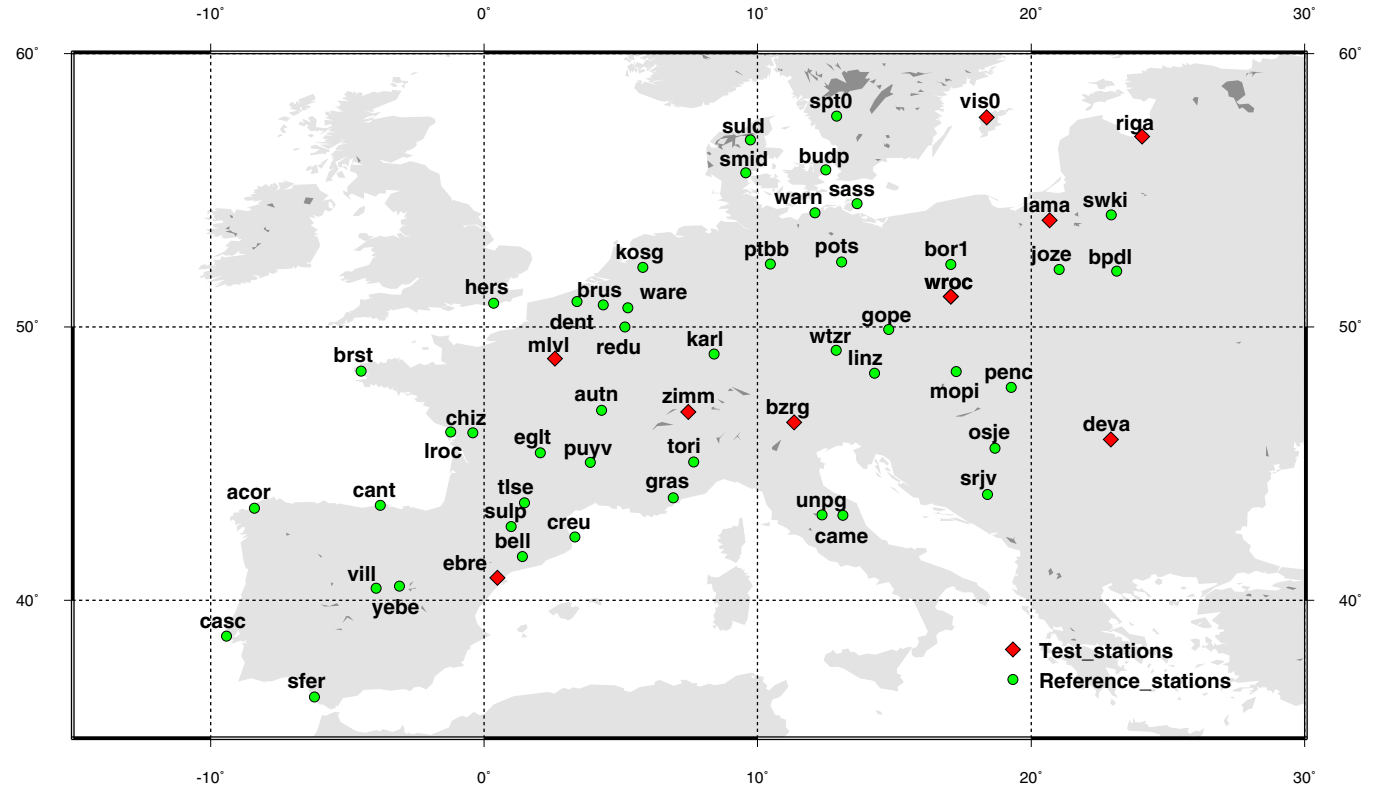

Fig. 2. Stations selected from EPN and their distribution. Green dots show the reference stations for the determination of SDED clocks. Red diamonds are the PPP test stations. (For interpretation of the references to colour in this figure legend, the reader is referred to the web version of this article.)

solutions for each station. In data analysis, data sampling is 30 s and elevation cut-off angle is set to 10°. Data processing is performed on a Linux personal computer with AMD Athlon Dual Core 1.1 GHz processor and 2 GB memory. For results validation, we first compare the computing time from our approach and other approaches. We then compare the estimated SDED clocks to the IGS final clocks. To assess the accuracy of the coordinates of the test stations, their daily estimates are used as the truth benchmarks instead of official coordinates from EUREF to avoid the potential biases (Geng et al., 2009).

5.1. SDED clock comparison

One very attractive point of our approach is the efficiency in the estimation of satellite clocks. Table 1 shows the processing time of the SDED approach, the traditional zero-difference (ZD) approach and the epoch-difference (ED) approach from Ge et al. (2009) and Chen et al. (2008, 2009). Table 1 illustrates that the SDED approach is able to process 9–10 epochs within 1 s, and it is almost 3 times faster than the ED approach and 90 times faster than traditional ZD approach. Furthermore, with the number of reference stations increasing, the parameter number remains almost the same in SDED approach, while it linearly increases in ED approach and it increases even more dramatically in ZD approach. It shows that SDED approach is much more efficient, especially for real-time applications.

Table 1
Total processing time and average processing time at each epoch (EPO time) based on our (SDED) approach, the epoch-difference (ED) approach and the traditional zero-difference (ZD) approach.

Approach	SDED	ED	ZD
Total time (s)	307	783	25,997
EPO time (s)	0.11	0.29	9.57

For the validation of the SDED clocks, we compare the estimated SDED clocks to the IGS one. The IGS SDED clocks are calculated from the IGS final clocks by forming satellite-difference, with PRN01 satellite as reference satellite, and epoch-difference. Fig. 3 shows the results of the comparison. The RMSs are calculated based on clocks of the whole day with different biases for each satellite being removed, as they can be absorbed by station clocks and ambiguities in PPP without affecting the satellite clock accuracy. Fig. 3 shows that satellite clock precision is better than 0.07 ns, in which more than 70% of the satellite clocks have a RMS less than 0.03 ns (i.e. 1 cm).

5.2. PPP results based on SDED clocks

Table 2 presents for each test station the distance to the nearest reference station, RMS of 2-h static PPP positions

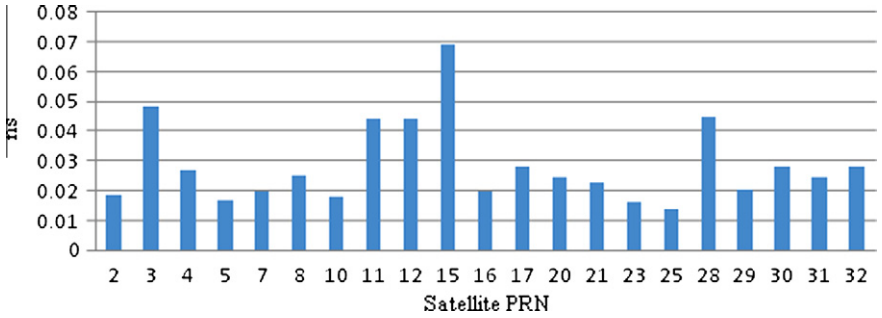

Fig. 3. RMS of the SDED clocks compared with that from the IGS.

Table 2
Distances to the nearest reference station, RMS (in cm) of 2-h static PPP coordinates with respect to the known coordinates in the North, East and Up directions in Network-PPP and Norm-PPP.

Stations	Distance (km)	Network-PPP			Norm-PPP		
		North	East	Up	North	East	Up
EBRE	115. 3	3.16	7.33	7.16	4.76	10.28	5.69
WROC	129.4	3.85	5.15	4.90	4.37	10.48	4.09
LAMA	159.5	2.11	3.76	5.75	4.51	8.81	6.39
MLVL	201.5	3.08	4.53	5.19	7.01	14.20	9.68
ZIMM	202.2	2.01	2.88	4.54	4.36	10.57	10.11
BZRG	221.3	3.27	7.31	6.79	4.44	13.96	8.88
RIGA	325.2	3.59	5.66	6.55	3.96	7.17	6.58
VIS0	326.6	2.11	3.72	5.03	4.26	7.02	6.58
DEVA	331.3	4.60	11.80	11.01	4.11	11.24	8.28
Mean	223.6	3.08	5.79	6.32	4.64	10.41	7.36

with respect to the truth benchmarks in Network-PPP and Norm-PPP. Network-PPP stands for PPP positioning where satellite clocks are estimated based on the reference network and the same IGU orbit is used as in the SDED clocks estimation. Norm-PPP stands for traditional PPP positioning where orbits and clocks are from the IGS final products. In Table 2, the test stations are arranged according to the distances column, the average distance is approximately 230 km.

Table 2 shows that with the distance to the nearest reference station up to 330 km, position RMS is still at cm level. In both solutions, accuracy in North direction is much better than East direction for all test stations, which can be explained that the pseudo-ambiguities in our modified PPP algorithm are not fixed. Comparing the results of Network-PPP to that of Norm-PPP, we see the mean position RMS improves from 4.64, 10.41, 7.36 cm to 3.08, 5.79, 6.32 cm in the North, East and Up directions, respectively, with a 3D mean accuracy improvement of 8.8%.

Daily kinematic PPP is performed for the selected stations and coordinates are compared with the benchmarks. Fig. 4 shows the residuals for the station WROC in Network-PPP case. The initial station coordinates differ from benchmarks by as much as 100 m. It takes around 1 h that few centimeters convergence in horizontal directions is reached. East component is worse than North component due to unresolved ambiguities. Some periodical effects can be noticed in height component, which maybe an impact of the PWC tropospheric model used in PPP.

Table 3 shows for all test stations the convergence time and the RMS of daily kinematic PPP positions with respect to the truth benchmarks in Network-PPP and Norm-PPP case. The convergence time is defined as that the difference from the benchmark of each coordinate component is less than 10 cm. The RMS is calculated from the kinematic coordinates after the convergence of the solution. As it shows that the current prototype system is not yet optimal, the convergence time is even more than 2 h for some stations. Nevertheless, it shows that the results of Network-PPP are better than Norm-PPP for all test stations.

Comparing the kinematic results of Network-PPP to that of Norm-PPP, we see the mean position RMS improves from 6.18, 7.53, 13.19 cm to 4.63, 5.82, 9.20 cm, with a 3D mean accuracy improvement of 5.2%.

From the PPP positioning results, we see that PPP positioning precision is at cm level for both Network-PPP and Norm-PPP, which demonstrates the capability of SDED clocks in user positioning. We also find obvious differences in the solution of Network-PPP and Norm-PPP. These difference, however, do not mean the accuracy of our estimated clocks is better than the IGS ones. Possible reasons are due to the facts that: (1) we are using a densified regional reference network rather than a global network, where user stations are less than 400 km apart

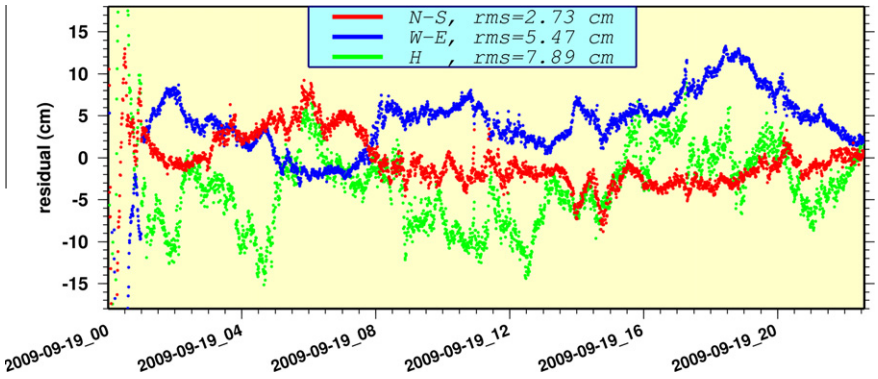

Fig. 4. Kinematic PPP solution of station WROC.

Table 3
Convergence time (CT) and RMS (in cm) of kinematic daily PPP coordinates with respect to the known coordinates in the North, East and Up directions in Network-PPP and Norm-PPP.

Stations	Network-PPP				Norm-PPP			
	CT (h)	North	East	Up	CT (h)	North	East	Up
EBRE	1.5	3.89	3.41	7.81	1.9	4.11	3.69	8.51
WROC	1.1	2.73	5.47	7.89	1.8	4.81	5.77	12.32
LAMA	2.5	5.64	5.89	10.12	2.9	6.50	7.04	12.49
MLVL	1.6	3.67	5.82	9.24	2.0	6.42	9.31	15.22
ZIMM	1.4	4.11	6.26	9.54	2.0	5.46	7.62	12.28
BZRG	1.4	4.37	7.76	7.52	1.6	6.56	9.98	15.93
RIGA	1.6	6.33	6.22	9.67	2.0	7.78	7.43	15.99
VIS0	1.4	5.79	6.83	9.41	2.0	6.31	7.84	12.92
DEVA	1.8	5.11	4.75	11.64	2.0	7.67	9.17	13.11
Means	1.6	4.63	5.82	9.20	2.0	6.18	7.53	13.19

from nearest reference station; (2) we use the consistent models in the step of "NET" and "PPP", therefore Network-PPP solutions are internally more consistent; (3) IGS final clocks are combined products from different analysis centers. The modeling and data handling strategies are different at each center and they are different to ours.

6. Conclusions and discussions

This study introduces a satellite- and epoch-differenced algorithm for fast estimation of satellite clocks and its application in PPP based positioning.

Based on the prototype system developed, we simulate a real-time experiment with data collected from EPN. The results show that our SDED approach is 3 times and 90 times faster than ED and ZD approach, respectively. As the parameters in our approach are satellite clocks only and thus do not increase with the expanding of reference network, whereas it increases in ED and ZD approach. Therefore, the improvement in computation efficiency will be even more dramatic when the network is bigger. The SDED clocks have a precision at the level of 0.1 ns compared to the IGS final clocks. By applying the SDED clocks, the 2-h static PPP positioning accuracy is 3.08, 5.79, 6.32 cm in the North, East and Up directions; the daily kinematic PPP positioning accuracy is at 4.63, 5.82, 9.20 cm.

The results from our prototype system are still not of the best quality, but it demonstrates the capability and benefits of the SDED approach. More efforts will be concentrated on the refinement of GNSS modeling and estimator of Kalman filter. Some more points should be studied in our approach, e.g. rapid convergence and PPP ambiguity fixing.

Acknowledgments

This research is supported by the National Natural Science Foundation of China (NSFC) (No. 40974018). We are grateful to two anonymous reviewers for their critical comments and helpful suggestions, which improved the manuscript greatly. The authors would like to thank the developers of the Generic Mapping Tools for providing GMT plotting tools. Thanks also go to the EUREF and IGS communities for the provision of GPS data and products.

References

Bock, Y., Nikolaidis, R.M., de Jonge, P.J., Bevis, M. Instantaneous geodetic positioning at medium distances with the Global Positioning System. Journal of Geophysical Research 105 (B12), 28233–28253, 2000.

Caissy, M. The IGS real-time pilot project – perspective on data and product generation, in: Streaming GNSS Data via Internet Symposium, 6–7 February, 2006.

Chen, J., Ge, M., Vennebusch, M., Deng, Z., Gendt, G., Rothacher, M. Progress of the real-time GNSS software development at GFZ, in: Oral Presentation at International GNSS Service Analysis Center Workshop, 2–6 June 2008, Miami Beach, Florida, USA, 2008.

Chen, J., Ge, M., Dousa, J., Gendt, G. Evaluation of EPOS-RT for real-time deformation monitoring. Journal of Global Positioning Systems 8 (1), 1–5, 2009.

Dousa, J. The impact of errors in predicted GPS orbits on zenith troposphere delay estimation. GPS Solutions, doi:10.1007/s10291-009-0138-z, 2009.

Dow, J., Neilan, R., Gendt, G. The International GPS service: celebrating the 10th anniversary and looking to the next decade. Advances in Space Research 36 (3), 320–326, 2005.

Feng, Y., Li, B. A benefit of multiple carrier GNSS signals: regional scale network-based RTK with doubled inter-station distances. Journal of Spatial Science 53 (2), P135–P146, 2008.

Ge, M., Chen, J., Gendt, G. EPOS-RT: software for real-time GNSS data processing, Geophysical Research Abstracts, vol. 11, EGU2009-8933, Oral Presentation at EGU General Assembly, 2009.

Geng, J., Teferle, F.N., Shi, C., Meng, X., Dodson, A.H., Liu, J. Ambiguity resolution in precise point positioning with hourly data. GPS Solutions 13 (4), 263–270, doi:10.1007/s10291-009-0119-2, 2009.

Han, S.C., Kwon, J.H., Jekeli, C. Accurate absolute GPS positioning through satellite clock error estimation. Journal of Geodesy 75, 33–43, 2001.

Hauschild, A., Montenbruck, O. Kalman-filter-based GPS clock estimation for near real-time positioning. GPS Solutions 13, 173–182, doi:10.1007/s10291-008-0110-3, 2009.

Hernandez-Pajares, M., Juan, J.M., Sanz, J., Orus, R., Garcia-Rodriguez, A., Colombo, O. Wide area real time kinematics with Galileo and GPS signals, in: Proceedings of the Institute of Navigation, Long Beach, California, 2004.

Janes, H.W., Langley, R.B., Newby, S.P. Analysis of tropospheric delay prediction models: comparisons with ray-tracing and implications for GPS relative positioning. Bulletin Géodésique 65, 151–161, 1991.

Kouba, J. A possible detection of the 26 December 2004 Great Sumatra–Andaman Islands earthquake with solution products of the international GNSS service. Studia Geophysica et Geodaetica 49 (4), 463–483, doi:10.1007/s11200-005-0022-4, 2005.

Rizos, C. Network RTK research and implementation: a geodetic perspective. Journal of GPS l.1 (2), 144–151, 2003.

Rocken, C., Mervart, L., Lukes, Z., Johnson, J., Kanzaki, M. Testing a new network RTK software system, in: Proceedings of GNSS 2004, Institute of Navigation, Fairfax, pp. 2831–2839, 2004.

Senior, K.L., Ray, J.R., Beard, R.L. Characterization of periodic variations in the GPS satellite clocks. GPS Solutions 12, 211–225, doi:10.1007/s10291-008-0089-9, 2008.

Xu, G. GPS : Theory, Algorithms and Applications, second ed Springer-Verlag, 2007.

Yang, Y. Robust estimation of geodetic datum transformation. Journal of Geodesy 73, 264–268, 1999.

Zumberge, J.F., Heflin, M.B., Jefferson, D.C., Watkins, M.M., Webb, F.H. Precise point positioning for the efficient and robust analysis of GPS data from large networks. Journal of Geophysical Research 102 (B3), 5005–5017, doi:10.1029/96JB03860, 1997.